

Metadata of the chapter that will be visualized online

Chapter Title	Reduced Order Lippmann-Schwinger-Lanczos Inverse Scattering Method	
Copyright Year	2025	
Copyright Holder	The Author(s), under exclusive license to Springer Nature Switzerland AG	
Author	Family Name	Baker
	Particle	
	Given Name	Justin
	Suffix	
	Division	Department of Mathematics
	Organization	University of Utah
	Address	Salt Lake City, UT, USA
	Email	
Author	Family Name	Cherkaev
	Particle	
	Given Name	Eleena
	Suffix	
	Division	Department of Mathematics
	Organization	University of Utah
	Address	Salt Lake City, UT, USA
	Email	
Corresponding Author	Family Name	Druskin
	Particle	
	Given Name	Vladimir
	Suffix	
	Division	Department of Mathematical Sciences
	Organization	Worcester Polytechnic Institute
	Address	Worcester, MA, USA
	Email	vdruskin@gmail.com
Author	Family Name	Moskow
	Particle	
	Given Name	Shari
	Suffix	
	Division	Department of Mathematics
	Organization	Drexel University
	Address	Philadelphia, PA, USA
	Email	
Author	Family Name	Zaslavsky
	Particle	
	Given Name	Mikhail
	Suffix	
	Division	Department of Mathematics
	Organization	Southern Methodist University
	Address	Dallas, TX, USA
	Email	

Abstract

The reduced Lippmann-Schwinger-Lanczos (LSL) algorithm, initially designed for two-dimensional (2D) inverse problems within the diffusion domain in the context of reduced-order modeling (ROM) (Baker et al., Regularized reduced order Lippmann-Schwinger-Lanczos method for inverse scattering problems in the frequency domain (submitted). arXiv:2311.16367v1) and later adapted to one-dimensional (1D) inverse scattering in the wave domain (Abilgazy and Zaslavsky, Lippmann-Schwinger-Lanczos approach for inverse scattering problem of Schrödinger equation in the resonance frequency domain. Extended abstracts of IPMS 2024 conference (accepted)), is extended in this work to address 2D Schrödinger inverse problems. Numerical experiments demonstrate that the required frequency sampling rate for 2D wave problems is substantially lower than for the 1D case, attributed to the inherently overdetermined nature of the 2D inverse problem. This finding suggests potential efficiency gains for solving high-dimensional wave-based inverse problems using reduced sampling strategies.

Keywords (separated by “ - ”)**Lippmann-Schwinger equation - Lanczos - Reduced order model****MSC 2020 (separated by “ - ”)****35R30 - 47A52 - 65N21 - 65F22 - 78A46**

Chapter 32

Reduced Order

Lippmann-Schwinger-Lanczos Inverse

Scattering Method

Justin Baker, Elena Cherkaev, Vladimir Druskin, Shari Moskow,
and Mikhail Zaslavsky

Abstract The reduced Lippmann-Schwinger-Lanczos (LSL) algorithm, initially designed for two-dimensional (2D) inverse problems within the diffusion domain in the context of reduced-order modeling (ROM) (Baker et al., Regularized reduced order Lippmann-Schwinger-Lanczos method for inverse scattering problems in the frequency domain (submitted). arXiv:2311.16367v1) and later adapted to one-dimensional (1D) inverse scattering in the wave domain (Abilgazy and Zaslavsky, Lippmann-Schwinger-Lanczos approach for inverse scattering problem of Schrödinger equation in the resonance frequency domain. Extended abstracts of IPMS 2024 conference (accepted)), is extended in this work to address 2D Schrödinger inverse problems. Numerical experiments demonstrate that the required frequency sampling rate for 2D wave problems is substantially lower than for the 1D case, attributed to the inherently overdetermined nature of the 2D inverse problem. This finding suggests potential efficiency gains for solving high-dimensional wave-based inverse problems using reduced sampling strategies.

Keywords Lippmann-Schwinger equation · Lanczos · Reduced order model

MSC 2020 35R30, 47A52, 65N21, 65F22, 78A46

J. Baker · E. Cherkaev

Department of Mathematics, University of Utah, Salt Lake City, UT, USA

V. Druskin (✉)

Department of Mathematical Sciences, Worcester Polytechnic Institute, Worcester, MA, USA

S. Moscow

Department of Mathematics, Drexel University, Philadelphia, PA, USA

M. Zaslavsky

Department of Mathematics, Southern Methodist University, Dallas, TX, USA

© The Author(s), under exclusive license to Springer Nature Switzerland AG 2025

A. Hasanov Hasanoğlu et al. (eds.), *Inverse Problems: Modelling and Simulation*, Research Perspectives Ghent Analysis and PDE Center 11,

https://doi.org/10.1007/978-3-031-87213-6_32



The inverse scattering problem formulated for the Helmholtz and Schrödinger operators has wide-reaching applications in fields such as quantum mechanics, remote sensing, geophysical, and medical imaging. Efficient numerical methods for inverse scattering have been developed in application to acoustic imaging, electromagnetic sensing, seismic exploration, and other fields. These methods include iterative techniques based on adjoint or backpropagation methods, Born and Rytov approximations, layer stripping methods, asymptotic methods for small volume inhomogeneities, Kirchhoff migration, and solving the Lippmann-Schwinger (LS) integral equation, see [7, 12, 14], also see a more recent review [13] and references therein discussing, in addition to the above mentioned techniques, far field and near field methods as well as phaseless recovery and nonlinear approaches. The problem is known to be severely ill-posed [6, 11].

Here, we use a truncated Lanczos representation to compute the data-driven internal solution of the PDE with unknown coefficients and then substitute it into the LS problem, thus effectively making it linear, as proposed in [9]; this results in the Lippmann-Schwinger-Lanczos (LSL) algorithm. The stability of projection subspaces in reduced order models (ROMs) is a critical concern, particularly when dealing with ill-posed problems. The sensitivity to data errors and potential nonphysical indefiniteness of the mass and stiffness matrices can lead to the loss of the Hamiltonian property in the reduced order system. To address this issue, two level ROM regularization via Gramian truncation is introduced in [3] to stabilize the LS algorithm. for the solution of the 2D inverse problem in the diffusion regime. The problem considered in [3] used a multiple-input multiple-output (MIMO) formulation corresponding to a symmetry preserving discretization of the 2D Neumann-to-Dirichlet (NtD) map. The LSL algorithm was extended to the wave domain for 1D inverse scattering problems [1] in single-input single-output (SISO) formulation, corresponding to the data given as a frequency-dependent 1D NtD a.k.a. scalar Weyl or transfer function. Here we apply the LSL algorithm to a 2D inverse problem in MIMO formulation for Schrödinger equation in the wave domain, which is a commonly used model in inverse scattering.

We note that the extension to a more general class of inverse problems may be possible with additional iterations [5], however, introducing iterations would compromise the advantages provided by direct inversion methods.

The LSL Method We consider the Schrödinger equation in a bounded domain Ω in \mathbb{R}^d , $d > 1$, with a smooth boundary $\partial\Omega$ at the wavenumber squared λ ,

$$\Delta u(x) + p(x)u(x) + \lambda u(x) = 0 \text{ in } \Omega, \quad \frac{\partial u}{\partial n} = g \text{ on } \partial\Omega. \quad (32.1)$$

The inverse scattering problem seeks identifying the nonnegative potential $p(x)$ using measured multifrequency Dirichlet data at a single or multiple receivers along the boundary, corresponding to a partial NtD map given by Neumann condition g .

Notice that we can rewrite the inhomogeneous Neumann boundary condition as the source $g(x)$ in the domain, assuming $g(x)$ is a compactly supported real

32 Reduced Order Lippmann-Schwinger-Lanczos Inverse Scattering Method

distribution localized near the boundary. A complete set of such distributions will 63 define the NtD operator, which is a tensor of order $2d - 2$ for every λ . Thus, the 64 inverse problem of determining $p(x)$ from the NtD given for a frequency interval 65 becomes overdetermined for $d > 1$. Denoting the operator in (32.1) as \mathcal{L} , we 66 (formally) represent the solution using the resolvent operator as 67

$$u = (\mathcal{L} + \lambda I)^{-1} g, \quad \text{where} \quad \mathcal{L} = -\Delta + pI \quad (32.2)$$

defined for functions on Ω satisfying the homogeneous Neumann boundary condition at $\partial\Omega$. The LSL method uses the values of the transfer function $F(\lambda)$ as the 68 data: 69

$$F(\lambda) = \langle g, u \rangle = \int_{\partial\Omega} g(x)u(x, \lambda)dx = \langle g, (-\Delta + pI + \lambda I)^{-1} g \rangle \quad (32.3)$$

The case with $d = 1$ considered in [1] corresponds to the Schrödinger equation 71 for a scalar function u in the domain $\Omega = (0, L)$, $0 < L < \infty$. The data for the 72 inversion are the values of the function $F(\lambda)$ and its derivative given for specific 73 $\lambda_j \in \mathbb{R}$, $j = 1, \dots, m$: 74

$$F(\lambda)|_{\lambda=\lambda_j} \in \mathbb{R}, \quad \frac{dF(\lambda)}{d\lambda}|_{\lambda=\lambda_j} \in \mathbb{R} \quad \text{for } j = 1, \dots, m. \quad (32.4)$$

The SISO inverse problem requires to determine $p(x)$ in (32.1) from the data (32.4) 75 with real or complex-valued function $F(\lambda)$ and correspond collocated receiver 76 and transmitter density $g(x)$ as given by (32.3). The MIMO formulation with 77 l collocated transmitter and receiver distributions g_i normally used for $d > 1$ 78 and usually corresponds to symmetric matrix valued function $F(\lambda) \in \mathbb{C}^{l \times l}$ with 79 elements 80

$$F_{ij}(\lambda) = \langle g_i, (-\Delta + pI + \lambda I)^{-1} g_j \rangle, \quad i = 1, \dots, l, \quad j = 1, \dots, l.$$

Normally g_i are chosen in such way, that $F(\lambda)$ becomes an approximation of the 81 NtD map. 82

In [3], the authors considered diffusion formulation with data on an interval 83 of \mathbb{R}_+ . Here we consider a wave formulation on the real negative interval $\lambda \in 84 [\lambda_{min}, 0] \subset \mathbb{R}_-$. The diffusion case corresponds to the Laplace transform of the 85 diffusion equation with exponential factor $e^{-\lambda t}$ with $\lambda > 0$. Our formulation in 86 the wave domain arises from the Fourier transform of the wave equation with the 87 time-dependent harmonic factor $e^{\pm i\omega t}$, where ω is the harmonic frequency of the 88 oscillation yielding $\lambda = -\omega^2$. Shifting from positive to negative intervals of λ 89 in wave problems produces images of significantly higher resolution, however it 90 requires different sampling strategies. 91

A positive interval lays outside of the spectrum of \mathcal{L} , and the choice of the 92 data points can be based, for example, on H_2 optimal points [4]. However, a large 93

enough negative interval contain the spectrum, so to accurately describe the transfer function, the data points should separate the spectral points, i.e., at least alternate with the spectral points. Density of spectral points can be estimated via Weyl's law

$$\lim_{\lambda \rightarrow \infty} \frac{N(\lambda)}{\lambda^{d/2}} = (2\pi)^{-d} \omega_d \text{vol}(\Omega), \quad (32.5)$$

where ω_d is the volume of the unit ball in \mathbb{R}^d . Here $N(\lambda)$ is the **number of the eigenvalues less than or equal to λ** . Generally, we choose density of sample points as $c \frac{d}{d\lambda} N(\lambda)$ with a moderate integer oversampling constant $c > 1$, that for $d > 1$ yields good results. To avoid overflow, we remove data points with absolute measurement values above certain threshold, that lay to close to the spectral points. We also note that inverse scattering problem in multi-dimensional case $d > 1$ is over-determined for MIMO scenario, so it is enough to use $c = 2$. In contrast, for 1D SISO problem values $c \geq 3$ are required for good reconstructions [1].

Lippmann-Schwinger Integral Equation If F_0 is the background transfer function corresponding to the solution u^0 for known p_0 , then the nonlinear Lippmann-Schwinger equation for the unknown function p can be written as

$$F_0 - F = \langle u^0, pu \rangle \quad (32.6)$$

where u is the (unknown) solution corresponding to the (unknown) coefficient p . One of the main difficulties of applying the LS approach to inverse problems is that this is a nonlinear equation. The LSL method [9] uses a (data-driven) approximate \tilde{u} of the solution u which is computed via Lanczos orthogonalization directly from the data without knowing p . This leads to the linear with respect to p equation: $F_0 - F \approx \langle u^0, p\tilde{u} \rangle$. This precomputing is based on embedding properties of the data-driven reduced order models (ROMs) developed in [8] and results in the linear system of equations for $p(x)$:

$$F_0(\lambda_j) - F(\lambda_j) = \int_{\partial\Omega} u_0(x, \lambda_j) \tilde{u}(x, \lambda_j) p(x) dx, \quad j = 1, \dots, m \quad (32.7)$$

LSL Algorithm A critical component of the LSL algorithm is computation of \tilde{u} , so we address it in more details. Let $u_j = u(x, \lambda_j)$ be solutions to (32.1) corresponding to $\lambda = \lambda_j$ for $j = 1, \dots, m$. We construct the Galerkin system that determines the data-driven Reduced Order Model (ROM) by projecting the problem (32.1) into the subspace V spanned by the functions $u_1(x), \dots, u_m(x)$,

$$(S + \lambda M)c = b. \quad (32.8)$$

Here the symmetric, positive definite stiffness and mass $m \times m$ block matrices 121
 respectively \mathbf{S} and \mathbf{M} with $l \times l$ blocks obtained from the data via Loewner algorithm 122
 [3–5, 10]: 123

$$M_{ij} = \frac{F(\lambda_i) - F(\lambda_j)}{\lambda_j - \lambda_i}, \quad M_{ii} = -\frac{dF}{d\lambda}(\lambda_i). \quad (32.9)$$

and 124

$$S_{ij} = \frac{F(\lambda_j)\lambda_j - F(\lambda_i)\lambda_i}{\lambda_j - \lambda_i}, \quad S_{ii} = \frac{d(\lambda F)}{d\lambda}(\lambda_i). \quad (32.10)$$

The right-hand side \mathbf{b} is a real vector of $l \times l$ blocks given by $F(\lambda_j)$. For any λ , 125
 the solution to (32.1) can be approximated by data-generated solution 126

$$u \approx \tilde{u} = V\mathbf{c} = V(\mathbf{S} + \lambda\mathbf{M})^{-1}\mathbf{b}, \quad (32.11)$$

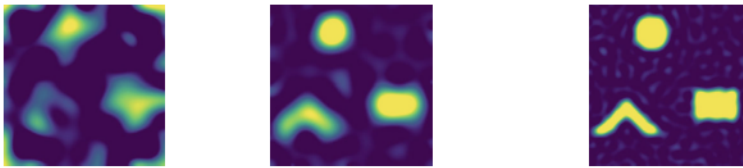
where V is an operator that can be represented via semi-infinite matrix $V \in \mathbb{R}^{\infty \times ml}$ 127
 with vector-columns from a Hilbert space given by orthogonalized background 128
 snapshots computed for $p \equiv 0$ at λ_i , $i = 1, \dots, m$. A key component of the data- 129
 driven ROM approach is asymptotic independence of the orthogonalized snapshots 130
 V on unknown $p(x)$, in spite of possibly strong dependence of the original snapshots 131
 u . This is thanks to the specially chosen orthogonalization algorithm via the block- 132
 Lanczos recursion with matrix $\mathbf{M}^{-1}\mathbf{S}$ and initial block-vector \mathbf{b} [5, 9]. Thus, all 133
 the parameters in the r.h.s. of (32.11) can be computed from the data, so we call \tilde{u} 134
 data-driven or data-generated solution. 135

To summarize, the LSL algorithm executes the following steps. The first step is 136
 constructing the data generated internal solution \tilde{u} via (32.11). The next step is to 137
 solve the linear system of Lippmann-Schwinger integral equations (a linear inverse 138
 problem). Indeed, use of $\tilde{u}(x, \lambda_j)$ instead of $u(x, \lambda_j)$ in the Lippmann-Schwinger 139
 integral equation produces a linear system for the unknown $p(x)$ given by (32.7). 140

The disadvantage of the LSL method is that improving the quality of the recon- 141
 structed solution requires increasing the number of frequencies. However, as the 142
 number of frequencies increases, the condition number of Loewner matrices \mathbf{S} and 143
 \mathbf{M} increases, and due to noisy data they can lose their positive-definiteness, leading 144
 to breakdown of the orthogonalization algorithm. To prevent this, a regularized 145
 (truncated) Reduced Order Model is constructed in [3] by projecting matrix pencil 146
 (\mathbf{S}, \mathbf{M}) onto the eigenvectors of \mathbf{M} corresponding to the real positive eigenvalues. 147
 Additional regularization is implemented to address intrinsic ill-posedness of 148

The regularized LSL algorithm provides an efficient approximation of the 149
 resolvent and results in a stable numerical algorithm. 150

Results of Numerical Simulations for the MIMO Problem Here, we present 2D 151
 results of numerical reconstructions of the perturbation composed of three shapes: 152
 a circle, a rectangle and a corner, embedded in homogeneous background $p_0 = 0$ 153



Born for $\lambda \in [-80; -2]$ Reconstruction for $\lambda \in [-80; -2]$ Reconstruction for $\lambda \in [-380; -2]$

Fig. 32.1 Shape perturbation reconstruction using the Born, and LSL methods

in $\Omega = [-1; 1]^2$. All three objects have the intensity $p = 1$, We considered MIMO 154 dataset with 8 collocated sources/receivers located on the boundary $\partial\Omega$ (2 per each 155 piece of boundary) and multiple frequencies. In Fig. 32.1 we plotted the results of 156 reconstructions for frequency range $\lambda \in [-80; -2]$ obtained by Born (left) and LSL 157 (middle) as well as by LSL for $\lambda \in [-380; -2]$. As one can observe, our approach 158 strongly overperforms Born for the same dataset. Also, adding higher frequencies 159 allowed to sharpen the image significantly. We also note that these reconstructions 160 are much sharper than the ones obtained in [3] for diffusion Schrödinger problem. 161

Conclusions The paper discusses the data-driven reduced Lippman-Schwinger- 162 Lanczos (LSL) method providing an efficient approach to inverse scattering for 163 multi-dimensional Schrödinger problem in a wave regime. The LSL is the direct 164 reconstruction algorithm that gives an explicit map between the ROM and the 165 unknown potential p ; it does not require an iterative numerical scheme. Other 166 advantages of the method are stability of the regularized ROM and construction of 167 the Galerkin ROM, exactly matching the data, directly from the data. Employing the 168 wave formulation allowed to sharpen the images compared to diffusion Schrödinger 169 problem [3]. We observed that the sampling rate can be significantly relaxed 170 compared to the 1D case [1]. We can speculate that such relaxation is possible thanks 171 to the overdetermined nature of the 2D formulation using frequency-dependent NtD 172 map, and probably even more sampling coarsening is expected for 3D problems. 173

Acknowledgments The authors acknowledge support from the Division of Mathematical Sci- 174 ences at the US National Science Foundation (NSF) through grants DMS-2008441, DMS- 175 2308200, DMS-2111117, DMS-2110773, DMS-2136198, DMS-2206171, and from the Air Force 176 Office of Scientific Research (AFOSR) through grants FA955020-1-0079 and FA9550-23-1-0220. 177

178

References

179

1. Abilgazy, A., Zaslavsky, M.: Lippmann-Schwinger-Lanczos approach for inverse scattering 180 problem of Schrödinger equation in the resonance frequency domain. Extended abstracts of 181 IPMS 2024 conference (accepted) 182

32 Reduced Order Lippmann-Schwinger-Lanczos Inverse Scattering Method

AQ3

- 2. Antoulas, A.C., Sorensen, D.C., Gugercin, S.: A survey of model reduction methods for large-scale systems. *Contemp. Math.* **280**, 193–219 (2001) 183
- 3. Baker, J., Cherkaev, E., Druskin, V., Moskow, S., Zaslavsky, M.: Regularized reduced order Lippmann-Schwinger-Lanczos method for inverse scattering problems in the frequency domain (submitted). arXiv:2311.16367v1 184
- 4. Beattie, C.A., Drmac, Z., Gugercin, S.: Quadrature-based IRKA for optimal H2 model reduction. In: 8th Vienna International Conference on Mathematical Modelling, IFAC-PapersOnLine, vol. 48, issue 1, pp. 5–6 (2015) 188
- 5. Borcea, L., Druskin, V., Mamonov, A.V., Moskow, S., Zaslavsky, M.: Reduced order models for spectral domain inversion: embedding into the continuous problem and generation of internal data. *Inverse Problems* **36**(5), (2019) 191
- 6. Cherkaev, E., Tripp, A. C.: Inverse conductivity problem for inaccurate measurements. *Inverse Problems* **12**(6), 869 (1996) 194
- 7. Colton, D., Kress, R.: *Inverse Acoustic and Electromagnetic Scattering Theory*, vol. 93. Springer, Berlin (2013) 196
- 8. Druskin, V., Mamonov, A.V., Thaler, A.E., Zaslavsky, M.: Direct, nonlinear inversion algorithm for hyperbolic problems via projection-based model reduction. *SIAM J. Imag. Sci.* **9**(2), 684–747 (2016) 198
- 9. Druskin, V., Moskow, S., Zaslavsky, M.: Lippmann-Schwinger-Lanczos algorithm for inverse scattering problems. *Inverse Problems* **37**(7), 075003 (2021) 201
- 10. Fletcher, C.: *Computational Galerkin Methods*. Springer, Berlin (1984) 203
- 11. Mandache, N.: Exponential instability in an inverse problem for the Schrödinger equation. *Inverse Problems* **17**, 1435–1444 (2001) 204
- 12. Nachman, A.I., Ablowitz, M.J.: A multidimensional inverse-scattering method. *Stud. Appl. Math.* **71**(3), 243–250 (1984) 206
- 13. Novikov, R.G.: *Multidimensional Inverse Scattering for the Schrödinger Equation. Mathematical Analysis, its Applications and Computation*, pp. 75–98. Springer, Berlin (2022) 208
- 14. Symes, W.W.: Reverse time migration with optimal checkpointing. *Geophysics* **72**(5), SM213–SM221 (2007) 210

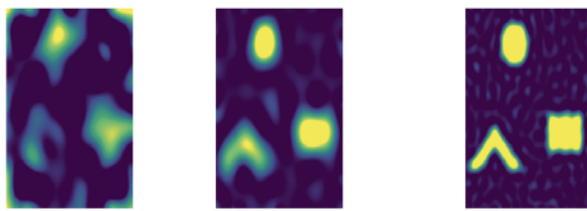
AQ4

AUTHOR QUERIES

- AQ1.** The citation of Refs. “[3] and [1]” are not allowed in the abstract section hence the same has been modified as per style. Please check, and correct if necessary.
- AQ2.** Please provide an update for Refs. [1] and [3].
- AQ3.** Ref. [2] is not cited in the text. Please provide the citation or delete it from the list.
- AQ4.** Please provide page range for Ref. [5].

Uncorrected Proof

Alternative Texts for Your Images, Please Check and Correct them if Required

Page no	Fig/Photo	Thumbnail	Alt-text Description
	Fig1	 Born for $\lambda \in [-80; -2]$ Reconstruction for $\lambda \in [-80; -2]$ Reconstruction for $\lambda \in [-380; -2]$	Three abstract images are displayed side by side. The first image, labeled "Born for $\lambda \in [-80; -2]$," shows a pattern of blurred, colorful shapes. The second image, labeled "Reconstruction for $\lambda \in [-80; -2]$," features similar shapes with slightly more defined edges. The third image, labeled "Reconstruction for $\lambda \in [-380; -2]$," presents distinct geometric shapes, including a circle, triangle, and rectangle, with clear boundaries. The color scheme includes shades of purple, blue, and yellow.